

# A PRACTICAL METHODOLOGY FOR ESTIMATING WAVE SPECTRA FROM THE SIR-B

A step-by-step procedure is outlined to convert synthetic aperture radar imagery into estimates of ocean surface-wave spectra. The procedure is based on a linearized version of a model that relates synthetic aperture radar image intensity spectra and wave slope- or height-variance spectra. The outlined procedure is applied to synthetic aperture radar imagery from the Shuttle Imaging Radar mission and is shown to produce spectra that, except in the lowest sea state, are highly correlated with two-dimensional spectra measured independently.

## INTRODUCTION

A number of investigators have demonstrated the general resemblance of synthetic aperture radar (SAR) image spectra and ocean-wave spectra.<sup>1-3</sup> Within certain limits, the wavenumber (or inverse wavelength) and propagation direction of ocean-wave systems derived from SAR image spectra have agreed well with independent measures of these parameters.

A more complete verification of the potential of spaceborne SARs to produce reliable wave-spectra estimates has awaited two developments: (a) alternative airborne techniques to estimate two-dimensional wave spectra with wavenumber and angular resolution comparable to those of SAR image spectra, and (b) an integration of various SAR wave-imaging theories into a procedure for converting SAR image spectra into estimates of ocean-wave slope- or height-variance spectra.

During the second Shuttle Imaging Radar (SIR-B) mission in October 1984, SAR imagery was acquired off the southern coast of Chile. Simultaneously, two-dimensional wave spectra were acquired by a NASA P-3 aircraft equipped with a radar ocean-wave spectrometer (ROWS)<sup>4</sup> and a surface contour radar (SCR).<sup>5</sup> Both instruments had been tested and verified in previous experiments.

In 1981, Alpers et al.<sup>6</sup> proposed a comprehensive approach to the interpretation of SAR image modulation in terms of ocean surface wave slope. A linearized and simplified version of the wave-imaging models detailed by Alpers et al. (see the article by Lyzenga preceding this one) was included in a proposed method by Monaldo

and Lyzenga<sup>7</sup> to convert SAR wave imagery into estimates of ocean-wave slope- and height-variance spectra.

In this article, we will review a practical procedure for converting SAR imagery to wave spectra, particularly emphasizing some of its still-uncertain aspects. We will also compare SAR wave spectra computed using this procedure with spectra estimated independently from the ROWS and SCR, thereby revealing both the potential and the limitations of the SAR to estimate wave spectra. Additional spectral comparisons from the SIR-B experiment are discussed in the article by Beal in this issue. Some early comparisons are also given in Beal et al.<sup>8</sup>

## WAVE-SPECTRA ESTIMATION PROCEDURE

A five-step procedure used to estimate wave slope- and height-variance spectra is shown schematically in Fig. 1.<sup>7</sup> The initial input is the two-dimensional SAR intensity image  $I(x,y)$ . When properly calibrated, image intensity is proportional to backscattered radar power. The digitally processed, geometrically and radiometrically corrected imagery used in this article has been provided by the Jet Propulsion Laboratory. The imagery is divided into image frames 512 by 512 pixels on a side. Each pixel corresponds to an area 12.5 by 12.5 meters on the surface, so that the entire image frame covers a 6.4- by 6.4-kilometer area.

Image normalization is performed by subtracting the mean image intensity and then dividing by this mean. The resulting normalized image is in units of fractional modulation. SAR wave-imaging theories are generally characterized in terms of fractional image modulation.

Fourier transformation of the image and squaring result in a level 1 spectrum,  $S_1(k_a, k_r)$ , where  $k_a$  is the azimuth (parallel to the satellite track) wavenumber and  $k_r$  is the range (perpendicular to the satellite track) wavenumber.

All imaging systems have finite resolution, and SARs are no exception. The effect of this finite resolution on SAR image spectra is to reduce spectral response at high



Frank M. Monaldo is a senior staff physicist in the Space Geophysics Group, The Johns Hopkins University Applied Physics Laboratory, Laurel, MD 20707.

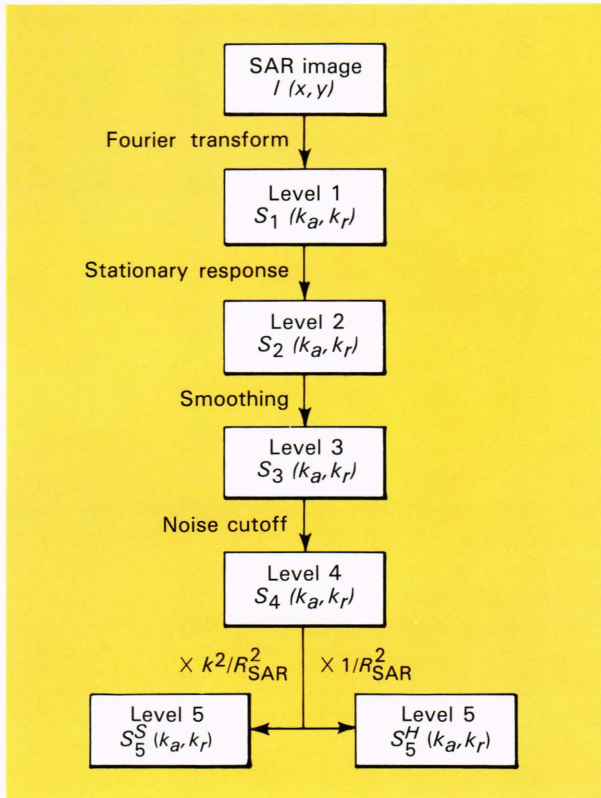


**Figure 1**—The procedure for calculating an ocean-wave spectrum from a SAR image. The SAR image,  $I(x,y)$ , is a map of the backscattered radar power as a function of the azimuth position,  $x$ , and the range position,  $y$ . A level 1 spectrum is generated by the Fourier transformation and squaring of a normalized SAR image. The level 2 spectrum is a correction of the level 1 spectrum for finite SAR resolution. By smoothing the level 2 spectrum, a more well-behaved level 3 spectrum is obtained. A noise level is subtracted from the level 3 spectrum, reducing the effect of speckle noise and yielding a level 4 SAR image spectrum. An estimate of the wave slope- or height-variance density spectrum, a level 5 spectrum, is produced by dividing the level 4 spectrum by the quantity  $R_{SAR}^2(k_a, k_r)$ , which is discussed in the text.

wavenumbers. The spectral density values at large wavenumbers are smaller than they would be in an infinite resolution system. Tilley<sup>9</sup> (see also Tilley, this issue) has been able to estimate and partially correct for this reduced response. A level 2 spectrum,  $S_2(k_a, k_r)$ , is produced by applying Tilley's "stationary response" correction to increase high-wavenumber spectral response.

The spectral estimate at each wavenumber bin located at any given  $k_a$  and  $k_r$  has only 2 degrees of freedom with an associated uncertainty of 100 percent and therefore is not very reliable statistically. To improve statistical reliability, a level 2 spectrum is smoothed with a Gaussian-weighted running average. The full width of the Gaussian kernel at the point where it falls to 60 percent of its maximum value is typically 7 wavenumber bins, about 0.007 rads per meter. The resulting smoothed spectrum is designated as a level 3 spectrum,  $S_3(k_a, k_r)$ .

Although the spectral estimate in any particular wavenumber bin in a level 3 spectrum is no longer independent of values in neighboring wavenumber bins,

it is far more statistically reliable. Each spectral estimate now has more than 100 degrees of freedom with an associated uncertainty of less than 10 percent. Others who process SAR imagery might prefer to use more or less averaging in the trade-off between statistical reliability and spectral resolution. Excessive smoothing will tend to distort the true spectral shape, particularly in the low-wavenumber regions of the spectrum.

Because SAR is a coherent imaging system, SAR imagery has the unfortunate quality that it is corrupted by multiplicative speckle noise. The amount of the noise depends on the number of looks used to form the image and on the mean and variance of the image. The speckle noise manifests itself in the SAR image spectrum as a white noise pedestal upon which the actual wave spectrum rests. The noise level of the pedestal, as predicted by Goldfinger,<sup>10</sup> is subtracted from the level 3 spectrum to generate a level 4 spectrum,  $S_4(k_a, k_r)$ . If  $N_0$  is this speckle noise level, then  $S_4(k_a, k_r) = S_3(k_a, k_r) - N_0$ . Any spectral value less than zero is set equal to zero.

A level 4 spectrum can be considered an *enhanced* SAR image spectrum. Up to this point, no model of the relationship between SAR image intensity modulation and ocean surface wave slope or height has been invoked. Using the imaging models developed by Alpers et al.<sup>6</sup> and linearized by Monaldo and Lyzenga,<sup>7</sup> a SAR modulation transfer function,  $R_{SAR}^2(k_a, k_r)$ , is used to convert a level 4 spectrum into a level 5 height-variance spectrum,  $S_5^H(k_a, k_r)$ , using

$$S_5^H(k_a, k_r) = \frac{S_4(k_a, k_r)}{R_{SAR}^2(k_a, k_r)}, \quad (1)$$

where

$$R_{SAR}^2 = \left[ \frac{R^2}{V^2} g \cos \theta \right] k k_a^2 + \left[ \frac{16 \cot^2 \theta}{(1 \pm \sin^2 \theta)^2} \right] k_r^2.$$

The angle  $\theta$  is the radar incidence angle with respect to nadir,  $R/V$  is the range-to-velocity ratio of the SAR platform,  $g$  is gravitational acceleration, the plus sign refers to vertical radar polarization, and the minus sign to horizontal polarization. Since the wave slope-variance spectrum is related to the height spectrum by  $k^2 (= k_a^2 + k_r^2)$ , a level 5 slope-variance spectrum is given by

$$S_5^S(k_a, k_r) = \frac{S_4(k_a, k_r) k^2}{R_{SAR}^2(k_a, k_r)}. \quad (2)$$

It is interesting to note that the  $k^2/R_{SAR}^2(k_a, k_r)$  is nearly constant over a broad range of wavenumbers, so that a level 4 spectrum should closely resemble a slope-variance spectrum.

## OCEAN-SURFACE MOTION

Because the SAR is a Doppler device, movement of the ocean surface affects the resulting SAR image. A

scatterer with a component of velocity in the radar look direction results in an azimuth displacement of the scatterer in the image by an amount proportional to the scatterer velocity and  $R/V$ , the range-to-velocity ratio of the SAR platform. The periodic shifting of scatterers by orbital velocities of the long (greater than 50 meters) azimuth-traveling ocean-surface waves is one mechanism by which azimuth-traveling waves are imaged by a SAR.<sup>6</sup> However, when velocities cause displacements in the image comparable to the ocean wavelength, or if the velocities are not highly correlated to the long wave, azimuth position shifts caused by surface velocities tend to degrade, rather than enhance, the SAR image.

The formally nonlinear remapping of the position of scatterers causes a smearing of the image in the azimuth direction and can be thought of as a loss of resolution in that direction.<sup>7,11</sup> The reduced azimuth resolution of a SAR image, like the effect of finite image resolution discussed earlier, results in a spectrum with reduced response at large azimuth wavenumbers. Attempts have been made, with some success, to correct for this dynamic response by procedures similar to the stationary response correction.<sup>11</sup> However, the correction schemes do not yet seem robust enough to be included here. For example, it is still not clear to us how the azimuth fall-off might affect the amount of speckle noise present and presumably to be subtracted in obtaining a level 4 spectrum. Nonetheless, in spite of difficulties, a dynamic response correction ought to be applied, if possible. In the following article, Tilley describes a more recent method, partially compensating for the lack of response at large azimuth wavenumbers.

Even with a dynamic response correction, an examination of SAR image spectra from Seasat and SIR-B has resulted in an empirical estimate of the minimum detectable azimuth wavelength,  $\lambda_m$ , given by

$$\lambda_m \sim \left(2 \frac{m^{1/2}}{s}\right) \frac{R}{V} H_s^{1/2}, \quad (3)$$

where  $H_s$  is the ocean significant wave height (SWH),<sup>7,8,11</sup> defined as four times the standard deviation of wave height with respect to the mean water level.

Interestingly, this limitation seems to be most severe in relatively mild sea states. Low sea states usually have dominant wavelengths short enough to be lost in the fall-off of azimuth response. In high sea states, although the minimum detectable azimuth wavelength,  $\lambda_m$ , increases, typical dominant ocean wavelengths are sufficiently long, at least at shuttle altitudes, to avoid the azimuth falloff problem. Since the effect is proportional to  $R/V$ , there is a strong argument in favor of reducing satellite altitudes for spaceborne SARs dedicated to measuring ocean-surface waves. Beal (this issue) discusses the implications of this performance limitation in more detail.

The low, 235-kilometer altitude of the SIR-B SAR turns out to have a  $\lambda_m$  smaller by a factor of nearly four than did the Seasat SAR. For example, Eq. 3 would predict a  $\lambda_m$  of 120 meters at a typical 3-meter SWH

sea state for the SIR-B SAR compared to 420 meters for the Seasat SAR, which orbited at 800 kilometers.

## COMPARISONS WITH INDEPENDENT SPECTRA

Comparisons of suitably corrected SAR wave spectra  $S_5^H(k_a, k_r)$  or  $S_5^S(k_a, k_r)$  with estimates of the wave spectra from the SCR and ROWS serve not only to confirm the potential for SAR measurement of waves but also to reveal some inherent limitations. SAR spectral data from SIR-B were acquired over five days, from October 8 to 12, 1984. We choose here to concentrate on the last three days, when the SAR signal-to-noise ratio was a minimum of 5 decibels.

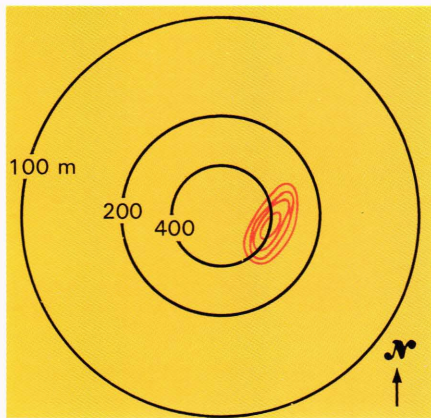
Figure 2 shows contour plots of three height-variance spectra on October 12, from the SCR, ROWS, and SAR. The center of the spectrum corresponds to zero wavenumber, and the outer circle corresponds to a wavenumber of  $2\pi/100$  radians per meter. Each contour corresponds to a constant spectral energy density. Peaks in the spectrum indicate concentrations of wave energy.

This day is particularly interesting in that the dominant 400-meter wave system traveled almost exactly along the azimuth. The imaging of azimuth traveling waves is perhaps less well understood than the imaging of range-traveling waves. Note that all three instruments clearly show the wave system at the same wavenumber and direction. It seems that shapes of the SAR and SCR spectral peaks are in best agreement, although all agree well.

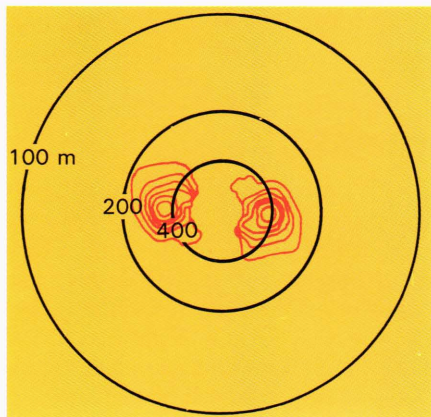
On October 11, because only a limited amount of SCR data were available, we compare only the ROWS and SAR slope-variance spectra in Fig. 3. In this case, there are two nearly range-traveling wave systems at wavelengths of 375 and 135 meters, respectively. The spectra were derived from areas coincident within 50 kilometers and were acquired within 3 hours. They show very good agreement. The wavelengths, propagation directions, shapes, and relative magnitudes of the two peaks are very similar.

Spectra from October 11 and 12 clearly demonstrate the SAR's ability to monitor both range- and azimuth-traveling wave systems. The spectral comparisons from October 10 illustrate the limitation caused by azimuth falloff associated with ocean-surface motion. Figure 4 shows height-variance spectra from ROWS, SCR, and SAR; the maximum wavenumber is  $2\pi/50$  radians per meter in these spectra. This mild, nearly 2-meter sea state shows some short small wavenumber peaks as well as an angularly broad wave system at wavelengths as short as 50 meters. The system is clearly present in the SCR and ROWS spectra. However, because much of the angular breadth of the spectrum extends in the SAR azimuth direction, the high azimuth wavenumber region of the broad wave system is abruptly cut off.

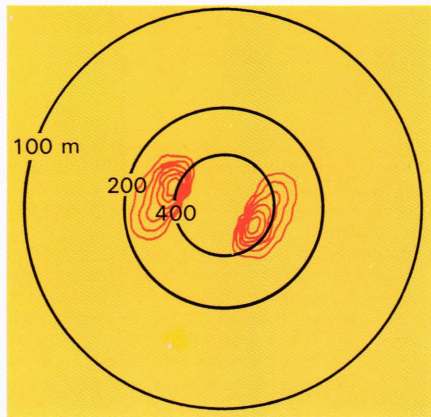
The spectra we have shown are all relative spectra, normalized to their maximum value, without absolute units attached to the contours. Although SAR imaging theories are probably not yet sufficiently well developed



SCR



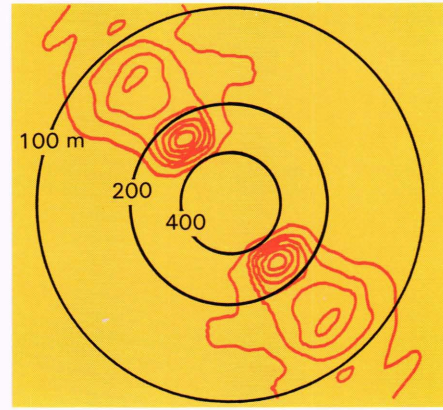
ROWS



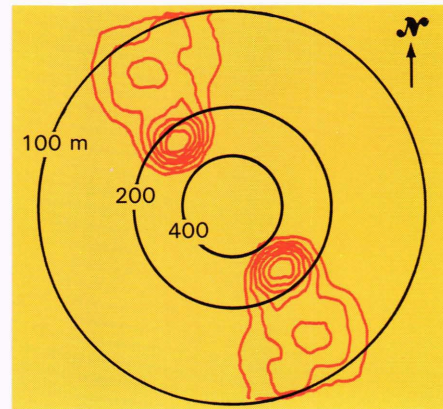
SAR

**Figure 2**—Wave height-variance density spectra for October 12, 1984. The SAR image ground track, i.e., the azimuth direction, is 11 degrees north of east. This day provides an example of accurate SAR imaging of azimuth-traveling ocean surface waves. The center of the spectrum corresponds to zero wavenumber or infinite wavelength. Except for the SCR spectra, there is a 180-degree ambiguity in the wave propagation direction.

that they can estimate slope- and height-variance spectra in absolute units with confidence, it is interesting to compare the SWH estimate from the SAR and other instruments aboard the P-3 aircraft. In addition to SCR and the ROWS on the P-3, a profiling lidar (airborne optical lidar) provided one-dimensional spectra, and a



ROWS



SAR

**Figure 3**—Wave slope-variance density spectra for October 11, 1984. The SAR image ground track, i.e., the azimuth direction, is 11 degrees north of east. This day provides an example of accurate SAR imaging of range-traveling ocean-surface waves.

nadir-looking altimeter of the advanced airborne flight experiment provided SWH estimates.

The integral of a two-dimensional height-variance spectrum over wavenumber space from either the SAR, SCR, or ROWS is equal to the total wave height variance VAR:

$$\text{VAR} = \int_0^\infty \int_0^\infty S_s^H(k_a, k_r) dk_a dk_r, \quad (4)$$

where, by definition,  $\text{SWH} = 4 \sqrt{\text{VAR}}$ .

Table 1 lists SWH estimates from the P-3 instruments and the SAR. For October 10, the SAR estimated the SWH at 1.3 to 1.4 meters, while the SCR and ROWS estimated slightly higher SWHs. Similarly, on October 11, the SAR modulation indicated an SWH between 3.2 and 4 meters, while all four other instruments had slightly higher estimates. On October 12, the SAR's SWH of 5.6 to 6 meters is a factor of two larger than the estimates by the other instruments. It is interesting to note that on October 10 and 11 much of the wave energy was traveling in the range direction. On October 12, the wave system was azimuth traveling. Apparently, the magni-

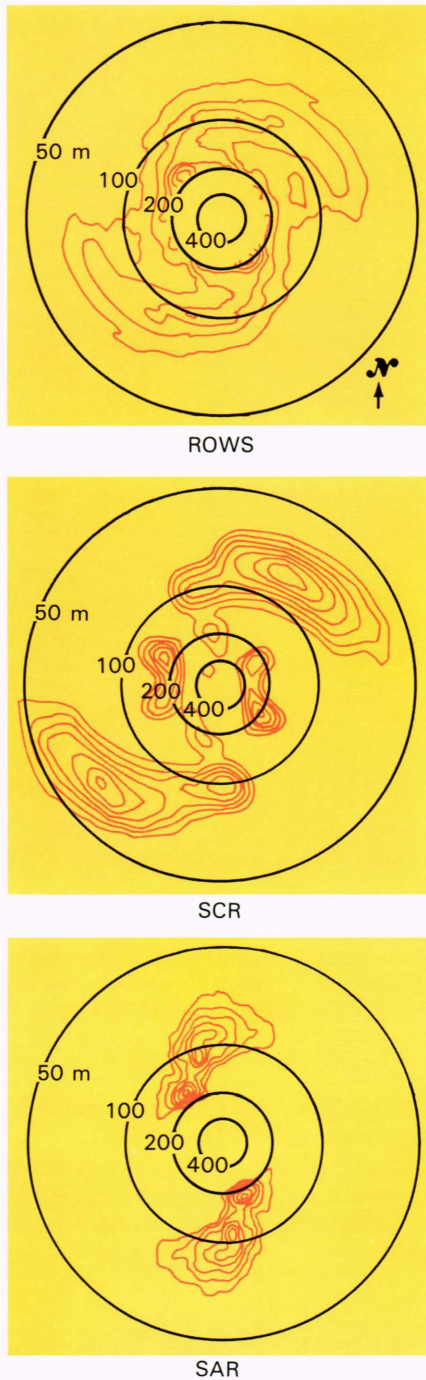


**Figure 4**—Wave height-variance density spectra for October 10, 1984. The SAR image ground track, i.e., the azimuth direction, is 11 degrees north of east. Note that these spectra (in contrast to Figs. 2 and 3) have a minimum displayed wavelength of 50 meters. Both the SCR and ROWS spectra show a very broad wave system whose dominant wavelength is about 70 meters. The SAR spectrum clearly exhibits a lack of response at high wavenumbers (shorter wavelengths) in the azimuth direction. The result is that the angular width of the 70-meter wavelength system appears greatly reduced.

tude of the component of our model for  $R_{SAR}(k_r, k_d)$  in the azimuth direction is a factor of two too small. On the other hand, the range component of the model appears slightly too large.

**Table 1**—SWH comparisons (meters).

Date	Shuttle	Aircraft Instruments			
	SAR	ROWS	SCR	AOL*	AAFE**
October 10	1.3 to 1.4	1.9	1.7	—	—
October 11	3.2 to 4.0	4.6	4.1	4.4	4.6
October 12	5.6 to 6.0	3.3	3.3	3.7	3.5

\* AOL = airborne optical lidar  
 \*\*AAFE = advanced airborne flight experiment (altimeter)

The fact that the SWH can be estimated this closely with SAR spectra is somewhat surprising and indicates that the linearized SAR imaging model is fairly good. Until we understand SAR modulation mechanisms more completely, relative SAR spectra will be more accurately normalized with SWH estimates from a radar altimeter.

**CONCLUSIONS**

A specific procedure for estimating slope- and height-variance spectra from SAR imagery has been developed and implemented that seems to produce relative spectra in close agreement with independently measured spectra. More work is required in specifying the exact magnitude of the SAR wave imaging function  $R_{SAR}^2(k_a, k_r)$ .

The most important limitation in SAR wave imagery is the lack of response at large azimuth wavenumbers caused by ocean-surface motion. Although this problem is partially correctable, low satellite orbits will be required to maximize the usefulness of ocean spectra derived from spaceborne SAR imagery.

**REFERENCES**

- R. C. Beal, D. G. Tilley, and F. M. Monaldo, "Large- and Small-Scale Spatial Evolution of Digitally Processed Ocean Wave Spectra from the Seasat Synthetic Aperture Radar," *J. Geophys. Res.* **88**, 1761-1778 (1983).
- R. C. Beal, T. W. Gerling, D. E. Irvine, F. M. Monaldo, and D. G. Tilley, "Spatial Variations of Ocean Wave Directional Spectra from the Seasat Synthetic Aperture Radar," *J. Geophys. Res.* **91**, 2433-2449 (1986).
- R. A. Shuchman, J. D. Lyden, and D. R. Lyzenga, "Estimates of Ocean Wavelength and Direction from X- and L-Band Synthetic Aperture Radar during the Marineland Experiment," *IEEE J. Oceanic Eng.* **OE-8**, 90-96 (1983).
- F. C. Jackson, W. T. Walton, and P. L. Baker, "Aircraft and Satellite Measurement of Ocean Wave Directional Spectra using Scanning-Beam Microwave Radars," *J. Geophys. Res.* **90**, 987-1004 (1985).
- E. J. Walsh, D. W. Hancock III, D. E. Hines, R. N. Swift, and J. F. Scott, "Directional Wave Spectra Measured with the Surface Contour Radar," *J. Phys. Oceanogr.* **15**, 566 (1985).
- W. Alpers, D. B. Ross, and C. L. Rufenach, "On the Detectability of Ocean Surface Waves by Real and Synthetic Aperture Radar," *J. Geophys. Res.* **86**, 6481-6498 (1981).
- F. M. Monaldo and D. R. Lyzenga, "On the Estimation of Wave Slope- and Height-Variance Spectra from SAR Imagery," *IEEE Trans. Geosci. Remote Sensing* (in press, 1986).
- R. C. Beal, F. M. Monaldo, D. G. Tilley, D. E. Irvine, E. J. Walsh, F. C. Jackson, D. W. Hancock III, D. E. Hines, R. N. Swift, F. I. Gonzalez, D. R. Lyzenga, and L. F. Zambresky, "A Comparison of SIR-B Directional Wave Spectra with Aircraft Scanning Radar Spectra and Spectral Ocean Wave Model Predictions," *Science* **232**, 1531-1535 (1986).
- D. G. Tilley, "Use of Speckle for Estimating Response Characteristics of Doppler Imaging Radars," *Opt. Eng.* **25**, 772-779 (1986).
- A. D. Goldfinger, "Estimation of Spectra from Speckled Images," *IEEE Trans. Aerosp. Electron. Syst.* **18**, 675-681 (1982).
- F. M. Monaldo, "Improvement in the Estimate of Dominant Wavenumber and Direction from Spaceborne SAR Image Spectra when Corrected for Ocean Surface Movement," *IEEE Trans. Geosci. Remote Sensing* **GE-22**, 603-608 (1984).